H-atom ionization by elliptically polarized microwave fields: Three-dimensional analysis

Krzysztof Sacha and Jakub Zakrzewski
Instytut Fizyki imienia Mariana Smoluchowskiego, Uniwersytet Jagielloński, ulica Reymonta 4, 30-059 Kraków, Poland
(Received 17 October 1997)

The classical analysis of H-atom ionization by elliptically polarized microwave fields is performed for a realistic three-dimensional model of an atom. As a limiting situation the circular polarization case is discussed in detail too. The sensitivity of initial electronic orbits of different orientation to microwave perturbation is studied analytically using the Chirikov overlap criterion. Generally the orbits lying in the polarization plane are most vulnerable to microwave perturbation, although important exceptions from this rule of thumb are found. In particular a class of orbits is found that is unusually stable against the perturbation. This behavior is linked to vanishing widths of the corresponding resonance islands within the first-order perturbation theory. The results of a recent experiment [Bellerman *et al.*, Phys. Rev. Lett. **76**, 892 (1996)] are qualitatively reproduced by the theory. [S1050-2947(98)05907-1]

PACS number(s): 32.80.Rm, 32.80.Wr, 32.80.Fb, 05.45.+b

I. INTRODUCTION

The ionization of hydrogen atoms by linearly polarized (LP) microwaves has been intensively studied for more than twenty years (for a recent review see [1]). Recently a considerable understanding of the phenomena induced by circularly polarized (CP) radiation has been also achieved [2,3]. By comparison, much less is known for a general case of elliptically polarized (EP) microwaves. The early studies [4–6] discussed the ionization threshold dependence on the microwave polarization in the regime of low frequencies (i.e., when the microwave frequency, $\omega \ll \omega_K$, where ω_K is the Kepler frequency corresponding to the initial atomic state). This domain of frequencies has been reexamined in a very recent experiment [7] showing a quite surprising sensitivity of the ionization yield to minute changes of the polarization. The experimental data have been reproduced fully by classical simulations.

The regime of high frequencies has been partially discussed within the framework of quantum localization theory using the so-called Kepler map [8]. This approach has been, however, questioned (at least for the limiting case of CP microwaves) by Nauenberg [9].

For most interesting moderate frequencies, when ω and ω_K are comparable in magnitude experimental data became also available [10]. The data show a surprising similarity in the ionization [11] threshold behavior as a function of the scaled frequency $\omega_0 = \omega/\omega_K$ for different microwave polarization (provided the microwave amplitude is appropriately rescaled), again reproduced by classical simulations. The results, obtained for $\omega_0 \in [0.6,1.4]$, i.e., in the broad neighborhood of the primary resonance between the driving field and the Kepler motion, may be, as briefly described by the authors of [10], understood by classical analysis of the pendulum Hamiltonian valid in the vicinity of the primary resonance.

The polarization of the microwave field becomes more important for higher ionization yields, when differently oriented initial states contribute (the initial sample of atoms having a well defined n_0 is a mixture of different angular quantum numbers in the experiment [10]). To understand this behavior one should not only consider initial states most vulnerable to perturbation but consider orbits of different angular momenta and orientations [12,13]. The results may be then also directly applicable to future experiments where, hopefully, initial states with all well-defined quantum numbers (n_0,l_0,m_0) will be prepared.

The general elliptical polarization case is highly nontrivial. For LP microwaves the conservation of the angular momentum projection onto the polarization axis, L_z, makes the dynamics effectively two dimensional. For the CP case while L_z is not conserved, the transformation to the frame rotating with the microwave frequency removes the explicit oscillatory time dependence [2]. Both these simplifications are no longer possible in the general EP microwave field and the problem becomes truly multidimensional, providing new challenges to the theory. Therefore, in a previous work [13] we have considered classically the threshold behavior in the simplified, two-dimensional (2D) model of an atom. The electronic motion has been limited, there, to the polarization plane.

The aim of this paper is to remove this limitation and consider classically a realistic fully three-dimensional (3D) atom. We consider the onset for the unbounded diffusion as determined by the Chirikov overlap criterion [14]. For initial orbits lying in the microwave polarization plane we recover the previous 2D results for both the CP [12] and EP [13] cases. Importantly, however, the 3D analysis provides additional understanding of the microwave-atom interaction.

The paper is organized as follows. In Sec. II we introduce the necessary notation and perform the resonance analysis. These results are then used in Sec. III for the discussion of the ionization threshold dependence on the shape and orientation of the initial electronic orbit. In particular, we concentrate on a family of states resistant to the microwave perturbation. A subset of such orbits has been already found in the 2D analysis [13]. We discuss also briefly the effect of the additional dimension on the classical predictions for the ionization threshold for the microcanonical sample of atoms based on the Chirikov overlap criterion (Sec. IV). The summary and the future perspectives form the content of the concluding part.

II. RESONANCE ANALYSIS OF THE SYSTEM

We shall consider a hydrogen atom perturbed by an elliptically polarized microwave field in the dipole approximation. The Hamiltonian (in atomic units) of the system reads

$$H=H_0+FH_1, \tag{2.1}$$

where

$$H_0=\frac{p_x^2+p_y^2+p_z^2}{2}-\frac{1}{\sqrt{x^2+y^2+z^2}}, \tag{2.2}$$

and

$$H_1=x\ \cos\ \omega t+\alpha y\ \sin\ \omega t. \tag{2.3}$$

F and ω denote the amplitude and the frequency of the microwave field, respectively. The degree of ellipticity is determined by α. In the limiting cases, $\alpha=0(\alpha=1)$ corresponds to a linear (circular) polarization of the microwave field. Expressing Eq. (2.3) as

$$H_1=\frac{1+\alpha}{2}(x\ \cos\ \omega t+y\ \sin\ \omega t)+\frac{1-\alpha}{2}(x\ \cos\ \omega t-y\ \sin\ \omega t) \tag{2.4}$$

allows us to visualize the interaction as being due to two CP waves, of different amplitudes (except for $\alpha=0$) rotating in the opposite sense.

As the next step we express the Hamiltonian, Eq. (2.1), in action-angle variables of the unperturbed Coulomb problem. We follow here the earlier treatments of the linear polarization [15] as well as the two-dimensional models for the CP [16,12] and the EP [13] cases with necessary modification. Due to its high symmetry, several choices are possible. The standard solution is to consider the canonically conjugate pairs (J,θ), (L,ψ), and (M,ϕ). J is the principal action (corresponding to the principal quantum number), related to the size of the ellipse. The corresponding angle, θ, determines the position of the electron on its elliptic trajectory. Its derivative $\dot{\theta}$ is the Kepler frequency $\dot{\theta}=\partial H_0/\partial J=1/J^3=\omega_K$. L is the angular momentum, ψ the angle of rotation around the axis defined by the angular momentum vector. Similarly, M,ϕ denote the projection of the angular momentum on the laboratory Oz axis and the angle of rotation around that axis, respectively. The high symmetry of the Coulomb problem is reflected by the fact that both ψ and ϕ are cyclic variables (the unperturbed Hamiltonian depends on J only).

The shape of the ellipse is best described by its eccentricity $e=\sqrt{1-L^2/J^2}$ while its orientation in the configuration space is determined by $(\phi,M/L,\psi)$. Define β via $\cos\beta=M/L$; β is the angle between the plane defined by the ellipse and the Oxy plane. In fact, (ϕ,β,ψ) are nothing but the Euler angles as defined by Goldstein [17] (with the notation change $\theta\rightarrow\beta$) if the unperturbed ellipse defines a local coordinate system with Oz' along the angular momentum vector and Ox' along the Runge-Lenz vector.

Then the unperturbed motion in the local coordinate frame may be expressed as a Fourier series [15]:

$$\begin{aligned}x'&=-\frac{3e}{2}J^2+2J^2\sum_{n=1}^{\infty}\frac{\mathcal{J}_n'(ne)}{n}\cos\ n\theta\\&=-\frac{3e}{2}J^2+\sum_{n=1}^{\infty}a_n\ \cos\ n\theta,\\ y'&=2J^2\frac{\sqrt{1-e^2}}{e}\sum_{n=1}^{\infty}\frac{\mathcal{J}_n(ne)}{n}\sin\ n\theta=\sum_{n=1}^{\infty}b_n\ \sin\ n\theta,\end{aligned} \tag{2.5}$$

where $\mathcal{J}_n(x)$ and $\mathcal{J}_n'(x)$ denote the ordinary Bessel function and its derivative, respectively.

The relations between the laboratory frame coordinates and the local frame related to the electronic ellipse allow us to express the Hamiltonian in action-angle variables. Eq. (2.1) becomes

$$H(\theta,J,\psi,L,\varphi,M,t)=H_0+FH_1, \tag{2.6}$$

where

$$\begin{aligned}H_0(J)&=-\frac{1}{2J^2},\\ H_1(\theta,J,\psi,L,\varphi,M,t)&=\frac{1+\alpha}{2}\sum_{n=-\infty}^{\infty}[V_n\cos(n\theta+\phi-\omega t)\\&\quad-U_n\sin(n\theta+\phi-\omega t)]\\&\quad+\frac{1-\alpha}{2}\sum_{n=-\infty}^{\infty}[V_n\cos(n\theta+\phi+\omega t)\\&\quad-U_n\sin(n\theta+\phi+\omega t)].\end{aligned} \tag{2.7}$$

Here, the Fourier expansion coefficients for $n=0$ are

$$\begin{aligned}V_0(J,L,\psi)&=-\frac{3e}{2}J^2\cos\ \psi,\\ U_0(J,L,M,\psi)&=-\frac{3eM}{2L}J^2\sin\ \psi,\end{aligned} \tag{2.8}$$

while those corresponding to $n\neq0$ are

$$\begin{aligned}V_n(J,L,M,\psi)&=\frac{J^2}{n}\left[\mathcal{J}_n'(ne)+\frac{M\sqrt{1-e^2}}{Le}\mathcal{J}_n(ne)\right]\cos\ \psi,\\ U_n(J,L,M,\psi)&=\frac{J^2}{n}\left[\frac{M}{L}\mathcal{J}_n'(ne)+\frac{\sqrt{1-e^2}}{e}\mathcal{J}_n(ne)\right]\sin\ \psi.\end{aligned} \tag{2.9}$$

The primary resonances for the perturbed motion satisfy

$$m\theta+\phi-\omega t=\text{const} \tag{2.10}$$

for the part of the perturbation proportional to $(1+\alpha)/2$ in Eq. (2.7), i.e., a right polarized circular wave, and

$$k\theta+\phi+\omega t=\text{const} \tag{2.11}$$

for the second part [proportional to $(1-\alpha)/2$, corresponding to the second, left circular polarized wave]. If one of these resonance conditions is satisfied, the second is also true, simultaneously; the electron interacts resonantly with both waves. Explicitly, for $J=J_m=(m/\omega)^{1/3}$ the m:1 resonance occurs due to the first part of the perturbation while the second resonance condition is met for $k=-m, \quad J_k=J_m$. Note that, for positive m and M the first resonance corresponds to the situation when the electronic motion projected onto the polarization plane rotates around the nucleus in the same sense as the first CP wave in Eq. (2.4). We shall call such a situation a ''corotating'' resonance, generalizing to 3D the description introduced for 2D problems [12,13]. Then the $k=-m<0$ condition merely expresses the fact that the same motion projected onto the polarization plane must rotate in the opposite sense to the second CP wave in Eq. (2.4) (the counter-rotating resonance). It was shown in [12,13] that in 2D the co-rotating resonances strongly affect the electronic motion while for the counter-rotating resonance the effect of the microwave perturbation is less pronounced. This is directly related to the form of Fourier coefficients, (2.9), where for $M>0$ the two terms in brackets have the same sign for $n>0$ and different signs for n negative.

Consider now a given m:1 resonance. In its vicinity one may apply the secular perturbation theory [18]. Making a canonical transformation to slowly varying variables

$$\hat{J}=J/m, \quad \Theta=m\theta-\omega t \tag{2.12}$$

allows us to average the Hamiltonian over the fast time variable [15,13]. Expanding simultaneously H_0 around the resonance values of the principal action $\tilde{J}=\hat{J}-\hat{J}_m$ with $\hat{J}_m=J_m/m$ and leaving the terms quadratic in $\tilde{J}$ transforms Eq. (2.6) into

$$\begin{aligned} H_{\rm res}=&-\frac{1}{2J_m^2}-\frac{\omega}{m}J_m-\frac{3m^2\tilde{J}^2}{2J_m^4}+F\frac{1+\alpha}{2}\{V_m\cos(\Theta+\phi)\\ &-U_m\sin(\Theta+\phi)\}+F\frac{1-\alpha}{2}\{V_{-m}\cos(\phi-\Theta)\\ &-U_{-m}\sin(\phi-\Theta)\}. \end{aligned} \tag{2.13}$$

The first term in $H_{\rm res}$ is the unperturbed energy, the second is a constant energy shift due to transformation (2.12) to the moving frame, the remaining terms constitute the secular motion Hamiltonian $\mathcal{H}_m$. The resonance island motion is described by $\tilde{J}$ and conjugate to it the angle Θ. A careful analysis of time scales [15] shows that $\phi, \quad \psi, \quad M, \quad L$ may change significantly over times $O(F^{-2})$. By comparison the motion in $\tilde{J}\Theta$ is much faster [with the period $O(F^{-1/2})$ [15]]. The former variables describe thus the initial elliptical trajectory, its shape (via the eccentricity $e=\sqrt{1-L^2/J_m^2}$) and its orientation in space. This allows one to cast $\mathcal{H}_m$ into the form of the pendulum Hamiltonian (after some algebra):

$$\mathcal{H}_m=-\frac{3m^2}{2J_m^4}\tilde{J}^2+F\Gamma_m(J_m,L,\psi,M,\phi;\alpha)\cos(\Theta-\delta), \tag{2.14}$$

where

$$\tan\delta=\frac{(1-\alpha)(V_{-m}\sin\phi+U_{-m}\cos\phi)-(1+\alpha)(V_m\sin\phi+U_m\cos\phi)}{(1-\alpha)(V_{-m}\cos\phi-U_{-m}\sin\phi)+(1+\alpha)(V_m\cos\phi-U_m\sin\phi)} \tag{2.15}$$

gives the center of the resonance island in Θ. δ is a constant up to first order in F, and may be incorporated into Θ by the shift of the origin. The strength of the resulting perturbation, $\Gamma_m(J_m,L,\psi,M,\phi;\alpha)$, is given by

$$\Gamma_m=\left\{\left(\frac{1+\alpha}{2}\right)^2[V_m^2+U_m^2]+\left(\frac{1-\alpha}{2}\right)^2[V_{-m}^2+U_{-m}^2]+\frac{1-\alpha^2}{2}[(V_mV_{-m}-U_mU_{-m})\cos 2\phi-(V_mU_{-m}+U_mV_{-m})\sin 2\phi]\right\}^{1/2}. \tag{2.16}$$

For circular polarization $\alpha=1$ and the above expression simplifies to

$$\Gamma_m=(V_m^2+U_m^2)^{1/2}, \tag{2.17}$$

becoming independent of ϕ, as expected.

For α arbitrary but restricting the electronic motion to the polarization plane we have $|M|=L$, thus $|V_m/\cos\psi|=|U_m/\sin\psi|=\mathcal{V}_n$ and

$$\Gamma_m=\left[\left(\frac{1+\alpha}{2}\mathcal{V}_m\right)^2+\cos 2(\psi+\phi)\frac{1-\alpha^2}{2}\mathcal{V}_m\mathcal{V}_{-m}+\left(\frac{1-\alpha}{2}\mathcal{V}_{-m}\right)^2\right]^{1/2}. \tag{2.18}$$

Here rotation around the Oz axis is equivalent to rotation around L, thus, say M and ϕ are redundant variables. Identifying $\psi+\phi$ with the global angle of rotation around Oz we recover the result found previously [13], Eq. (2.17).

The pendulum Hamiltonian (2.14) with the explicit form of the perturbation, Eq. (2.16), constitute the main analytical results of this work. They form the basis of the physical interpretation presented in the remaining sections.

III. CHIRIKOV RESONANCE OVERLAP ANALYSIS

The Hamiltonian, Eq. (2.14), together with Eq. (2.16) allows for a direct application of the Chirikov overlap criterion [14] to estimate the threshold for the unbounded diffusion for a given (with well-defined orientation and angular momentum) initial orbit. The criterion says that the chaotic unbounded diffusion (leading to high excitation and eventually ionization of our system) may take place when two neighboring resonances overlap. For $m:1$ and $m+1:1$ resonances, together with the heuristic ''2/3'' rule, which allows one to estimate the influence of higher-order resonances [14,18], we obtain

$$F_c(L,\psi,M,\phi;\alpha,m)=\frac{[(m+1)^{1/3}-m^{1/3}]^2}{3[(m+1)^{2/3}\sqrt{\Gamma_{m+1}}+m^{2/3}\sqrt{\Gamma_m}]^2}\,\omega^{2/3} \tag{3.1}$$

for the threshold microwave amplitude. This gives an analytic lower bound for the unbounded chaotic diffusion starting somewhere on the border between $m:1$ and $m+1:1$ resonances.

It is important to realize that once this diffusion is possible the electron will eventually ionize, i.e., there are no further bottlenecks for the excitation process. The reason for it is simple, the electron gains energy, the Coulomb force becomes weaker while the microwave perturbation becomes relatively stronger (with the fixed value of F) [19]. The perturbative, first order in F, approach yielding to Eq. (2.14) is no longer valid and, in particular, the adiabatic parameters determining the initial electronic orbit are no longer approximately constant. But our aim is not to accurately describe the details of this excitation process but merely to give the estimate for its onset for a given initial orbit. And that is provided by Eq. (3.1).

It is worthwhile, however, to understand the limitations of such a procedure. We consider here a multidimensional system; the phase space is seven dimensional. Therefore, the Arnold diffusion [18] may lead to excitation (and ionization) of the atom even for very weak microwave amplitudes, below the Chirikov threshold. The Kolmogorov-Arnold-Moser (KAM) tori does not divide the phase space, while the Chirikov criterion gives the estimate for the diffusion ''across the resonances,'' the Arnold diffusion ''along the resonances'' is always present. One may question therefore the usefulness of the Chirikov criterion for the estimation of ionization thresholds. However, in real experiments [1,10] the microwaves interact with atoms for a relatively short time of the order of a few hundred microwave periods. The Arnold diffusion process, on the other hand, is quite slow [18,20]. It has been shown, moreover, that it slows down significantly in the vicinity of KAM tori [21]. Therefore, only the diffusion ''across the resonances,'' taken into account by the Chirikov criterion, may lead to ionization in realistic interaction times.

On the other hand, for the very same reason, namely, the finite interaction time, the estimates based on the Chirikov criterion must be treated with caution. Close to the threshold for the unbounded diffusion, the transport in the phase space may be significantly slowed down due to several bottlenecks such as cantori [23]. Thus even above the onset of the chaotic motion very long times may be required for high excitation or ionization of atoms. Numerical estimates have shown that the classical ''ionization threshold'' may significantly decrease with increasing interaction time [22].

Keeping all that restrictions in mind, it is still worthwhile to use the Chirikov criterion with the understanding that it yields the qualitative trends rather than the quantitative predictions. For example, while for experimental interaction times the criterion will generally underestimate the threshold, it should, however, help to understand which initial orbits are most vulnerable to the perturbation as well as which orbits can stand quite strong microwave fields.

As mentioned above for $\alpha=0$ the microwave field becomes linearly polarized. We do not discuss this case here since the LP case has been covered substantially in the 2D study [13]. The results in 3D are practically the same as the projection of the angular momentum on the polarization axis is conserved. They become exactly equivalent for $M=0$ while the generalization to $M\neq 0$ is simple. On the other hand we commence the discussion of the results with the circular polarization comparing the 3D predictions with previously reported 2D analysis [12].

For the presentation of the results we used scaled variables defining scaled angular momentum $L_0=L/J$ and the scaled projection on the Oz axis $M_0=M/J$. Similarly the microwave field amplitude (and frequency) is scaled as $F_0=FJ^4(\omega_0=\omega/\omega_K=\omega J^3)$. This is possible due to typical classical scaling present in the Coulomb problems and is commonly used in microwave ionization studies [1,8]. For simplicity we drop in the following the subscript 0 since we shall always consider the scaled variables.

A. Circular polarization

For the CP case $\alpha=\pm 1$ and one of the two CP waves in Eq. (2.4) vanishes. Consider $\alpha=1$. Then orbits with $M>0$ will be corotating with the field while $M<0$ will correspond to orbits counter-rotating with respect to (w.r.t.) the microwaves. The results for $\alpha=-1$ may be recovered from those for $\alpha=1$ by reversing the direction of the angular momentum vector of the orbit (in particular by $M\rightarrow -M$ interchange), thus in the following we consider $\alpha=1$ only.

As mentioned above, the resonant interaction strength (2.17) depends on two of the Euler angles β,ψ only for CP microwaves. For $\beta=0$ we recover the 2D system, the electronic ellipse lies in the polarization plane and the dependence on ψ also disappears, as expected from the rotational symmetry of the microwave field.

Consider first the corotating orbits. In 2D [12] the lowest threshold for the unbounded diffusion as given by the Chirikov criterion is obtained for medium eccentricity ($e\approx 0.8$) orbits. Slightly higher threshold values are obtained for more elongated orbits with the eccentricity close to unity.

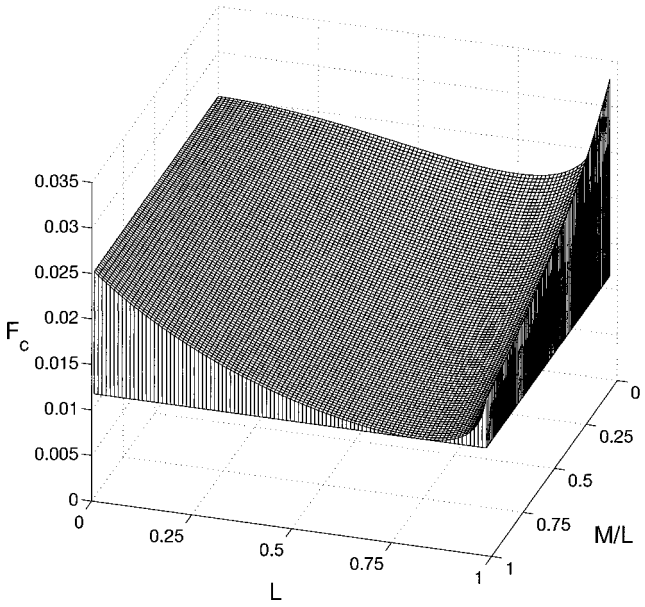

FIG. 1. The critical scaled microwave amplitude value, F_c [Eq. (3.1)] predicted by the Chirikov criterion for the overlap between $m{:}1$ and $m+1{:}1$ resonances for $m=1$ in the plane of the scaled angular momentum L and the inclination of the orbit as given by M/L for $\psi=0$. The microwaves are circularly polarized.

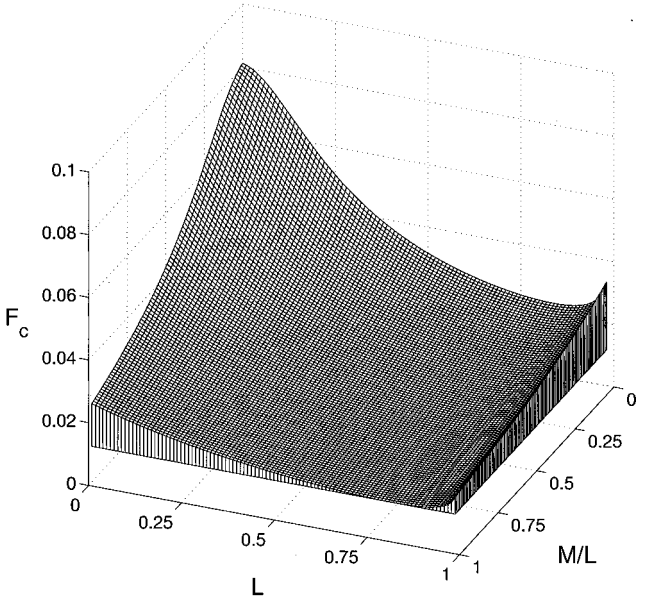

FIG. 2. Same as Fig. 1 but for $\psi=0.4\pi$, i.e., in the vicinity of the singular point $\psi=\pi/2$. Note the maximum in the threshold centered at $L=0$, $M/L=0$. The large microwave amplitude is required for the overlap because the effective perturbation strengths Γ_m of the resonances for low L and M/L values and ψ close to $\pi/2$ are very small. For such ellipses their projection on the polarization plane (and, thus the projection of the Fourier components of the perturbation, directly responsible for the effective interaction) reduces to the point centered at origin. The microwaves are circularly polarized.

The behavior of the low eccentricity orbits is markedly different. The electronic motion on the circular $(e=0)$ orbit is harmonic. In effect all primary resonances $m{:}1$ with $m\neq 1$ do not exist (have zero width), the corresponding V_m and U_m coefficients, compare Eq. (2.9), of the perturbation (with arbitrary microwave polarization) vanish. That implies that the Chirikov criterion diverges. The first-order perturbation theory is thus not sufficient to describe the behavior of such orbits and one should, in principle, use the higher orders in the analysis.

The crucial point is to realize that extremely small first-order resonance widths provide already an interesting qualitative picture (and, as mentioned above, only the qualitative predictions may be obtained using the Chirikov analysis). Since primary resonances disappear and regular structures in the phase space may be affected by higher-order terms in the perturbation, orbits with such properties will be more stable against the perturbation and can resist higher microwave amplitudes. We shall use this argument frequently in the following discussion, especially in the treatment of ''counter-rotating'' resonances.

As qualitative as they sound the above predictions agree very well with results of numerical simulations for circular orbits (compare Fig. 1 in [24]) where the rapid increase of the threshold around the scaled frequency $\omega_0=\omega/\omega_K=3$ has been observed. This correlates well with the divergence of the Chirikov criterion for the overlap between $2{:}1$ and $3{:}1$ resonances for circular orbits.

It is interesting to see how this picture is modified by extending the model to a real 3D world. As mentioned in the Introduction an intuition says that the orbits lying in the polarization plane will be most vulnerable to the perturbation. This picture is generally correct as shown in Fig. 1. Observe, however, that a high resistivity of circular orbits, even those lying in the polarization plane, results in the fact that medium eccentricity orbits inclined w.r.t. the polarization plane have a threshold lower than that corresponding to low eccentricity orbits lying in the plane. Thus the intuitive picture can be made more precise by saying that among all orbits of the same eccentricity those lying in the polarization plane will be most vulnerable to the microwave perturbation.

In a full 3D model not only the inclination of the orbit w.r.t. the polarization plane (i.e., $\cos\beta=M/L$) but also the orientation of the orbit (given by ψ) becomes important—compare Eq. (2.17). Generally $\psi=0$ corresponds to the lowest while $\psi=\pi/2$ to the highest threshold values for eccentric orbits (the sensitivity to ψ disappears of course for circular orbits).

This is exemplified in Fig. 2. Observe that the threshold rises for elongated orbits (small L) strongly inclined w.r.t. the polarization plane. This is understandable, the interaction between the electronic motion and the microwave field vanishes in the first order when the projection of the orbit on the polarization plane degenerates into the point. That happens for elongated orbits and $\psi=\pi/2$. Figure 2 represents the Chirikov overlap thresholds for $\psi=0.4\pi$ to avoid the divergence of the first-order theory at $\psi=\pi/2$.

To obtain quantitative predictions in the domain of small widths of primary resonances one should go to higher orders. This is beyond the scope of the paper. Qualitatively it is reasonable to assume that the regions of small Γ_m will be more stable against the perturbation. Still the absolute numbers obtained in the first order for the threshold microwave amplitude in the vicinity of Chirikov overlap criterion divergence should be treated with extreme caution.

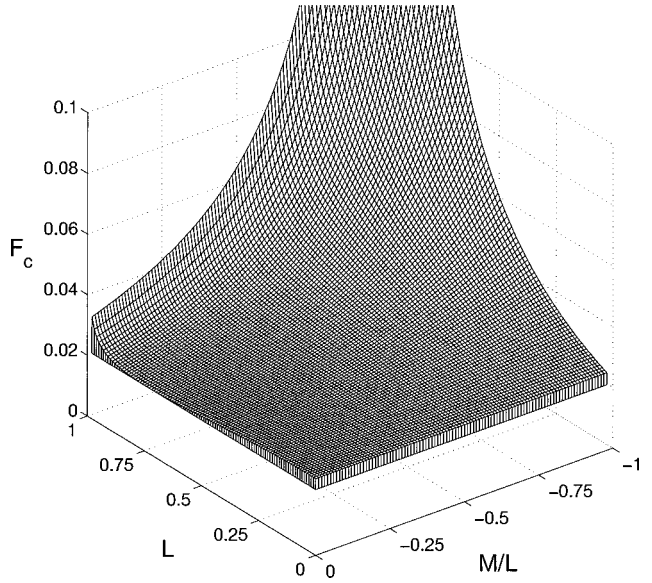

FIG. 3. The critical scaled microwave amplitude value, F_c [Eq. (3.1)], predicted by the Chirikov criterion for the overlap between m:1 and $m+1$:1 resonances for $m=1$ in the plane of the scaled angular momentum L and the inclination of the orbit as given by M/L for $\psi=0$. Note that M/L takes now negative values (counter-rotating case). The microwaves are circularly polarized.

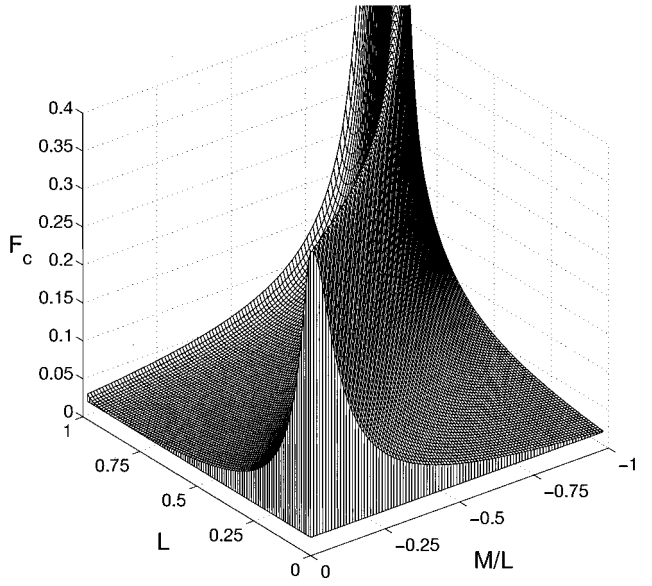

FIG. 4. The critical scaled microwave amplitude value, F_c [Eq. (3.1)], predicted by the Chirikov criterion for the overlap between m:1 and $m+1$:1 resonances for $m=1$ and $M<0$ (counter-rotating case) in the plane of the scaled angular momentum L and the inclination of the orbit as given by M/L for $\psi=0.48\pi$. The ridge of the threshold is given approximately by Eq. (3.2) for $m=1$. The divergence of the prediction occurs for $\psi=\pi/2$ thus the plot is presented for slightly different ψ values. The microwaves are circularly polarized. See text for the discussion.

Let us now discuss the counter-rotating orbits (M negative). They have in 2D much higher threshold for the unbounded diffusion than the co-rotating orbits [12]. For such orbits an inclination w.r.t. the polarization axis typically *lowers* the threshold as depicted in Fig. 3. Observe that the inclination of the orbit has the strongest effect for low eccentricity orbits. Already Nauenberg [9] in his 2D map analysis of the CP problem noticed the stability of circular orbits (in the counter-rotating case) and mentioned that this stability is removed by considering the 3D problem. This particular result nicely agrees with the $L\to 1$ limit in Fig. 3 (keeping in mind that again the Chirikov criterion strictly diverges in 2D for $L=1$ case for the reasons discussed above).

The most surprising and interesting is the fact that the very same stability does not fully disappear in 3D. To look for stability one should consider, as before, the minima of Eq. (2.17). For the counter-rotating case $M<0$ and the minimal $\Gamma_m=0$ is obtained, after inspection of Eq. (2.9), for $\psi=\pi/2$ (which makes V_m vanish) with a simultaneous condition

$$\frac{M}{L}\mathcal{J}_m'(me)+\frac{\sqrt{1-e^2}}{e}\mathcal{J}_m(me)=0, \tag{3.2}$$

coming from the condition for U_m in Eq. (2.9). Note that the similar factor in V_m is always positive (for $e>0$), thus $\psi=\pi/2$ is necessary to nullify also V_m. Condition (3.2) is weakly dependent on the resonance number m, thus the Chirikov criterion will yield a double peak structure [13] as a function of M/L or $L=\sqrt{1-e^2}$, each peak coming from a vanishing width of one of the two resonances that overlap. For ψ slightly detuned from the $\psi=\pi/2$ value the double-peak first-order structure disappears and we obtain a smooth ridge of increased stability. This is exemplified in Fig. 4 for the overlap between 1:1 and 2:1 counter-rotating resonances. Using the Taylor series for Bessel functions for small values of the argument one can easily verify that the condition (3.2) reduces, for small e (and both resonances), to $M/L\propto-\sqrt{1-e^2}+O(e^2)$. Thus, approximately, the stability condition is equivalent to saying that the projection of the orbit onto the polarization plane is a circle (at least for small eccentricity orbits). For high eccentricity, the stability peaks tend to the origin in $(L,M/L)$ plane—i.e., to the case when the projection onto the polarization plane reduces to the point.

Clearly the stability of the circular orbit in the counter-rotating 2D case is a limiting case of the ''stability family'' represented in Fig. 4. In this sense the Chirikov criterion helps us to verify and explain early remarks of Nauenberg [9].

While we present graphically the results for $m=1$ only very similar predictions are obtained for overlaps between m and $m+1$ resonances for $m>1$ (i.e., for higher frequencies). The condition (3.2) is valid for arbitrary m but is only weakly dependent numerically on m. This indicates that the stability family persists in a broad frequency range (the higher the resonance number m, the higher the scaled frequency as may be seen from the transformation to slowly varying variables in the previous section).

B. Elliptical polarization

Consider now the general case of elliptical polarization. Due to the competition between two circular waves rotating in the opposite sense [compare Eq. (2.4)] the effective resonant perturbation strength (2.16) is much more complicated

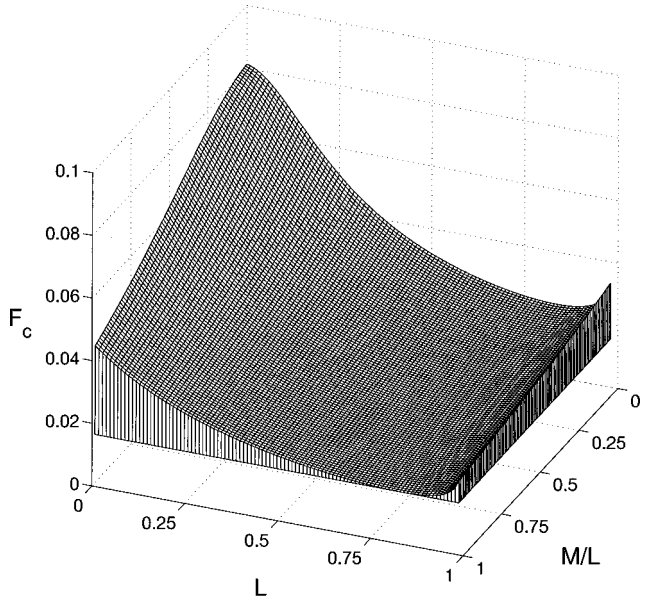

FIG. 5. Elliptically polarized microwaves with the ellipticity parameter $\alpha=0.5$. The critical scaled microwave amplitude value, F_c [Eq. (3.1)], predicted by the Chirikov criterion for the overlap between m:1 and $m+1$:1 resonances for $m=1$ in the plane of the scaled angular momentum L and the inclination of the orbit as given by M/L. Other Euler angles determining the electronic orbit orientation are $\psi=0.4\pi$ and $\phi=0$.

and depends on all three Euler angles corresponding to the electronic ellipse viewed in the laboratory frame. Let us first briefly summarize the 2D results [13].

For corotating orbits the threshold now depends on the mutual orientation between the polarization ellipse and the electronic ellipse, given (in the present 3D notation) by $\psi+\phi$. It has been found that the lowest thresholds are obtained when the major axes of the polarization ellipse and the electronic ellipse coincide, while the highest occur for the mutually perpendicular major axes. This condition directly follows from Eq. (2.18) and is independent of the ellipticity parameter α. On the other hand the sensitivity to the mutual orientation of ellipses depends on α and is the strongest for α small (almost linear polarization). This is obvious, for CP the orientation of the electronic ellipse plays no role (in 2D).

For the counter-rotating orbits in 2D a first-order resonant perturbation may vanish for $\psi+\phi=\pi/2$ and eccentricities depending on α and weakly on the resonance number m. In effect a double-peak structure threshold dependence on eccentricity (or angular momentum) is found. As in the case discussed previously, the two peaks correspond to vanishing Γ_m for each of the two resonances considered for the Chirikov criterion.

Of course the distinction between corotating and counter-rotating cases disappears for $\alpha=0$, i.e., for the linear polarization of microwaves.

The analysis of the orbits in 3D can be carried out in analogy to the easier CP case discussed above. Again, for a given eccentricity corotating orbits, the orbits lying in the polarization plane have the lowest Chirikov threshold. Additionally the resonant perturbation may vanish if the projection of the electronic ellipse on the polarization plane reduces to the point. Representative results are shown in Fig. 5.

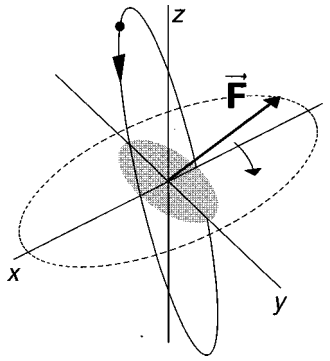

FIG. 6. Visualization of the situation leading to a vanishing width of the resonance island corresponding to the m:1 resonance. The solid line ellipse represents the approximation to the electronic motion as given by the mth Fourier component in the expansion (2.5). The black dot is the current position of the particle, the arrow indicates the direction of the motion. The shaded ellipse is the projection of this component on the polarization plane Oxy and it has the same eccentricity as the polarization (dashed) ellipse. Note that the electric field vector F and the projection of the electronic motion rotate in the opposite directions.

It is much more fruitful to inspect the threshold for counter-rotating orbits, where for a given resonance the perturbation may vanish in nontrivial situations. Inspecting the derivation of Eq. (2.16) it is easy to check that the exact conditions for minimizing Γ_m are obtained in the following steps:

(1) Take the Fourier component driven by a given resonance in Eq. (2.5), this is an ellipse centered around the origin lying in the $Ox'y'$ plane with main axes a_m and b_m.

(2) Project this Fourier component ellipse on the polarization plane Oxy.

(3) Vanishing Γ_m are obtained if the resulting projection, also an ellipse, has the major axis perpendicular to the major axis of the polarization axis and the eccentricities of both these ellipses are the same.

The corresponding situation is visualized in Fig. 6.

Since a_m and b_m in Eq. (2.5) depend on the resonance number m, the Chirikov criterion for the overlap between m and $m+1$ resonance will diverge for two close orientations of electronic ellipses. Therefore, it is more interesting, as before, to look at situations slightly ''detuned'' from the optimal, i.e., when both Γ_m and Γ_{m+1} are very small. Examples of such situations are presented in Figs. 7–9.

Figure 7 represents a situation similar to that shown already for CP in Fig. 4 but for EP case with $\alpha=0.5$. As before, instead of taking $\psi=\pi/2$, a value leading to the divergence, we consider a slightly different orientation of electronic ellipses, $\psi=0.48\pi$. The divergence of the threshold occurs when

$$\frac{M}{L}=-\frac{b_m}{\alpha a_m} \quad \text{for} \quad m=1 \quad \text{or} \quad m=2 \tag{3.3}$$

is satisfied for $\psi=\pi/2$. To make the third condition in the list above apparent, Eq. (3.3) may be expressed as

$$\alpha=-\frac{b_m}{a_m\cos\beta}. \tag{3.4}$$

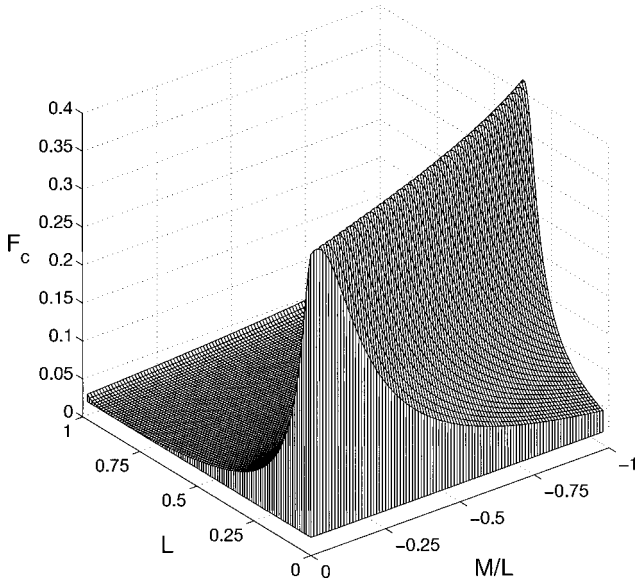

FIG. 7. Elliptically polarized microwaves with the ellipticity parameter $\alpha=0.5$. The critical scaled microwave amplitude value, F_c [Eq. (3.1)], predicted by the Chirikov criterion for the overlap between m:1 and $m+1$:1 resonances for $m=1$ and $M<0$ (counter-rotating case) in the plane of the scaled angular momentum L and the inclination of the orbit as given by M/L. Other Euler angles determining the electronic orbit orientation are $\psi=0.48\pi$ and $\phi=0$.

Either of these two conditions (i.e., for $m=1$ or $m=2$) describes approximately the ridge shown in the figure.

The predictions for the threshold depend on all the Euler angles describing the orientation of the electronic ellipse for EP case. In effect the position of the stability ridge is also affected by ϕ. Figure 8 presents the example. Note that the location of the ridge in the $(L,M/L)$ plane depends on ϕ. The divergence of the Chirikov threshold happens for $\psi=\phi=\pi/2$ and when

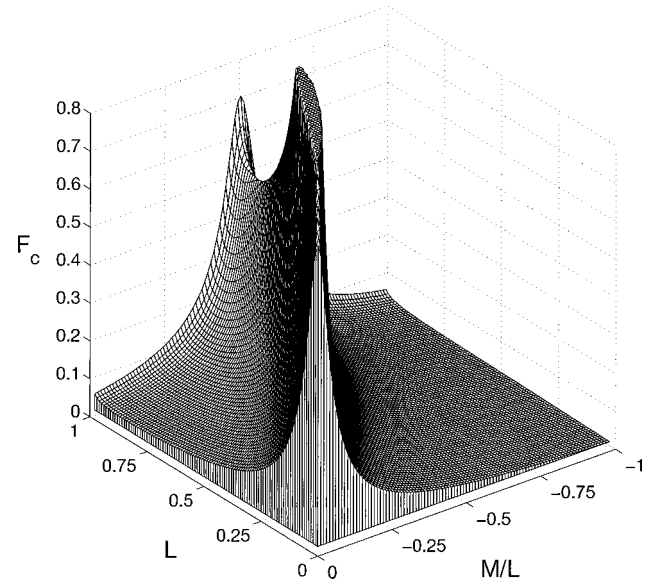

FIG. 8. Same as Fig. 7 but for $\phi=0.48\pi$, for the discussion see text.

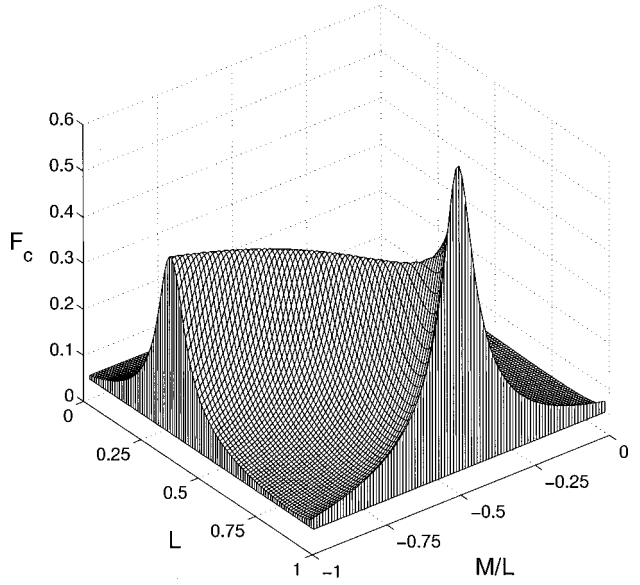

FIG. 9. Same as Fig. 7 but for $\phi=0.48\pi$ and $\psi=0$, for the discussion see text.

$$\alpha=-\frac{a_m\cos\beta}{b_m}, \tag{3.5}$$

as another example of the rules given above.

The rules does not require ψ to be close to $\pi/2$ to observe the increased stability as in the cases shown above. The necessary ellipse (or rather its projection orientation) may be obtained by adjusting ϕ. As an example consider Fig. 9 for which the stability ridge may be described approximately by

$$\alpha=-\frac{b_m\cos\beta}{a_m}. \tag{3.6}$$

For smaller α, i.e., when polarization of microwaves is closer to being linear, stable families of orbits converge to the situation resembling those for LP case. Here, in the limit $\alpha=0$, the distinction between corotating and counter-rotating trajectories disappears, a first-order theory predicts that orbits lying in the plane perpendicular to the polarization axis are stable. In effect the ridge moves with α (compare Fig. 9 with Fig. 10).

Finally let us mention that in the 2D restricted analysis [13] we have suggested that the existence of orbits resistant to the perturbation may allow one to produce electronic states of a given eccentricity by adjusting the microwave polarization and amplitude in such a way so as to ionize most of the microcanonical sample leaving only atoms with the chosen e value of the initial state. If possible, such a method would be a crude and cheap way of creating atoms in Rydberg states of well-defined angular quantum numbers supplementing other, more elegant but quite complicated in realization methods [25]. The present analysis, carried out in a full 3D model, shows that the states (orbits) that may survive the microwave pulse are not those of fixed eccentricity but rather those with a fixed eccentricity of their projection on the plane of polarization.

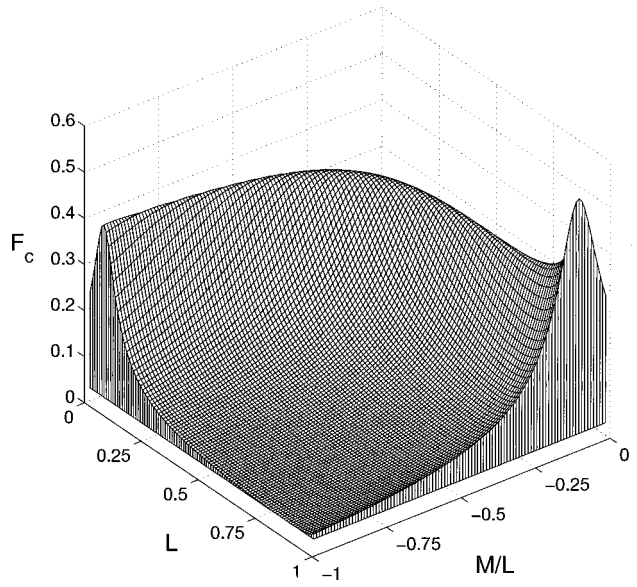

FIG. 10. Same as Fig. 9 but for $\alpha=0.1$, i.e., elliptical polarization closer to the linear polarization case, for the discussion see text.

IV. MICROCANONICAL SAMPLE CONSIDERATIONS

In the current experiments [10] initial atomic states entering the microwave cavity do not have well-defined quantum numbers except for the principal quantum number n_0. Classically that corresponds to a microcanonical sample of initial trajectories. Therefore, the results presented above cannot be directly compared with the experimental data.

One way of performing such a partial comparison is to minimize the classical threshold over all possible orientations and shapes of initial electronic ellipses of a given energy. Such a classical Chirikov overlap threshold has been used in [10]. The advantage of such a definition is its simplicity. On the other hand, such an approach cannot describe the ionization yield as a function of the microwave field amplitude.

The experimental thresholds are defined as the microwave amplitude at which a given $s\%$ ionization yield is obtained, the data are presented for 10% and 50% yields in [10]. An interesting quantity is then the ratio of thresholds for different polarizations. Denote by $R_L(s\%)=F^{\mathrm{LP}}(s\%)/F^{\mathrm{CP}}(s\%)$ the ratio of the scaled LP microwave amplitude leading to $s\%$ yield to the corresponding amplitude for the CP field. Similarly let $R_E(s\%)=F^{\mathrm{EP}}(s\%)/F^{\mathrm{CP}}(s\%)$, where $\alpha=0.263$ as in [10] for the EP microwave field. As found experimentally [10] $R_L(10\%)=1.41$ and $R_E(10\%)=1.26$.

By making an average over initial trajectories it is possible to make a theoretical estimate of these quantities using the Chirikov overlap criterion. The corresponding yields are obtained by finding the microwave amplitude at which the Chirikov overlap threshold is at least reached for a given $s\%$ of microcanonically distributed trajectories. Such a procedure has been carried out in the 2D case in [13] and compared with the numerical estimates (which simulated the microwave pulse shape according to [10] in 2D). The Chirikov overlap ratios in 2D overestimated the numerical values, both the numerical and Chirikov R_L and R_E decreased with $s\%$ (for the details of the comparison see [13]).

The similar approach is possible also in 3D and the resulting Chirikov overlap predictions are presented in Fig. 11. The experimental values are taken from Fig. 3 of [10] by averaging the data for scaled frequencies $\omega_0\in(1.05,1.2)$ (for higher ω_0 no data for elliptical polarization are available). The dotted lines in Fig. 11 represent the trends for R_L and R_E described in [10]: they remain approximately constant up to $s\%=30\%$ while for higher $s\%$ both quantities decrease due to the increase of CP thresholds.

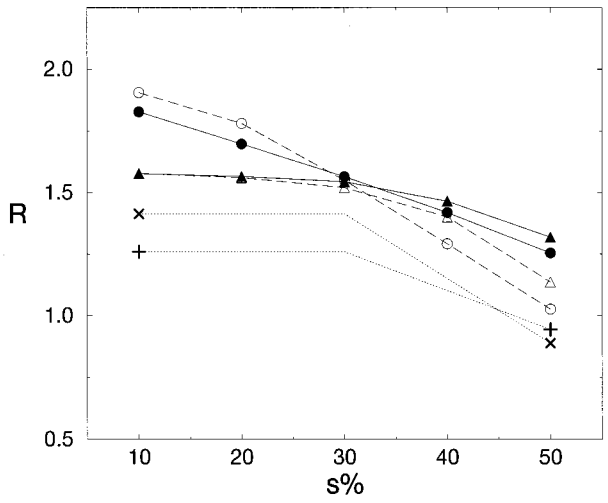

FIG. 11. The ratio of LP microwave amplitude to CP microwave amplitude, both leading to $s\%$ ionization yield, denoted as R_L and the similar ratio for EP microwaves with $\alpha=0.263$ to CP amplitude, R_E, as a function of $s\%$. Full circles (triangles) correspond to R_L (R_E) obtained from Chirikov overlap criterion in the present work using a full 3D microcanonical ensemble. Open symbols represent the results of 2D Chirikov analysis and are taken from [13]. Plusses and crosses represent the experimental values while the dotted lines show the intermediate trend as described in [10]. While Chirikov threshold numerical values are different from those obtained experimentally and by numerical simulation in 3D [10], present 3D results are less sensitive to $s\%$, especially for EP, in qualitative agreement with the experiment. For a further discussion see text.

Observe that the difference between 2D and 3D Chirikov predictions are quite small for 10% threshold and do not agree with the experimental data. We do not compare with numerical values in 3D since such calculations have been already performed in [10], and as we understand, reproduce the experiment quite well. Still the 3D Chirikov predictions while overestimating the experimental values quite well represent the dependence of R_L and R_E on $s\%$. This points to the importance of the full 3D analysis for reproducing experimental results.

One reason for the discrepancy between the Chirikov predictions and the experimental results may be due to the fact that the former consider a fixed amplitude of the microwaves while in the latter a smooth microwave pulse of rather short (154 cycles) duration has been used. As discussed in [13] the difference between a long time (Chirikov) prediction and the finite time simulation/experiment may indicate the sensitivity of the speed of the phase space transport to the microwave polarization.

V. SUMMARY AND CONCLUSIONS

We have considered the ionization thresholds, or more precisely the onset for the unlimited diffusion in the phase

space for the fully three-dimensional hydrogen atom illuminated by elliptically polarized microwaves. The effective resonant Hamiltonian valid in the first order in microwave amplitude F has been derived analytically, see Eqs. (2.14)–(2.16). That in turn has led to an analytical expression for the threshold microwave amplitude (3.1) coming from the overlap of two nearby resonances.

These expressions have been used to investigate the dependence of the classical threshold on the orientation and shape of initial electronic orbits. A comparison with earlier studies in two-dimensional atomic models confirmed that 2D restricted approximations are quite useful as far as the minimal thresholds for a given orbit shape are considered provided the orbits are of the corotating type, i.e., the electronic motion when projected on the polarization plane rotates in the same direction as the electric field does. On the other hand, inclined counterrotating orbits have lower thresholds than those lying in the polarization plane. In effect studies of ensemble of orbits (see last section as an example) require a full 3D treatment.

We have paid particular attention to orbits for which a first-order perturbation term vanishes. Such orbits can still ionize due to higher order in F effects but for them the real threshold is expected to be much higher than for other orbits. Examples of several families of such orbits have been identified and the conditions that they must fulfill have been given. By changing the ellipticity of the microwaves, described by α we may consider the limiting situations of a circular ($\alpha=1$) or linear ($\alpha=0$) polarizations. The families of stable (in the first order in F) orbits reduce in the well-understood case of LP polarization to orbits lying in the plane perpendicular to the polarization axis. For other microwave polarization two cases are possible. A very intuitive one is the case when the projection of the orbit on the polarization plane reduces to the point centered at origin. A less trivial condition occurs for counter-rotating orbits only, namely, the projection of the resonantly driven Fourier component of the orbit (generically an ellipse) must have a major axis perpendicular to the major axis of the polarization ellipse and the same eccentricity. The families of resistant orbits discussed here reduce, in the 2D limit, to the orbits identified and tested in [13].

The existence of orbits resistant to the perturbation indicates a mixed character of the phase space of atom + microwave field problem even at relatively high scaled fields. This indicates that the mechanism of transport in this system is highly nontrivial.

Finally let us mention that the resonance analysis presented here may be used for semiclassical quantization of states located in the corresponding resonance islands. Such an approach is well known for one-dimensional driven systems [26], the present analysis makes possible its extension to multidimensional systems, in particular a realistic microwave driven hydrogen atom. Work in this direction is in progress.

ACKNOWLEDGMENTS

We thank Dominique Delande for discussions. The support by the Polish Committee of Scientific Research under Project No. 2P03B 01413 (K.S.) and 2P03B 03810 (J.Z.) is acknowledged. K. Sacha acknowledges financial support from the Foundation for Polish Science.

[1] P. M. Koch and K. A. H. van Leeuwen, Phys. Rep. **255**, 289 (1995).
[2] J. Zakrzewski, R. Gębarowski, and D. Delande, Phys. Rev. A **54**, 691 (1996), and references therein.
[3] D. Delande and J. Zakrzewski, in *Classical, Semiclassical and Quantum Dynamics in Atoms*, edited by H. Friedrich and B. Eckhardt, Lecture Notes in Physics No. 485 (Springer, Berlin, 1997).
[4] P. Fu, T. J. Scholz, J. M. Hettema, and T. F. Gallagher, Phys. Rev. Lett. **64**, 511 (1990).
[5] T. F. Gallagher, Mod. Phys. Lett. B **5**, 259 (1991).
[6] J. A. Griffiths and D. Farrelly, Phys. Rev. A **45**, R2678 (1992).
[7] M. R. W. Bellermann, P. M. Koch, and D. Richards, Phys. Rev. Lett. **78**, 3840 (1997).
[8] G. Casati, I. Guarneri, and D. L. Shepelyansky, IEEE J. Quantum Electron. **24**, 1420 (1988).
[9] M. Nauenberg, Europhys. Lett. **13**, 611 (1990).
[10] M. R. W. Bellermann, P. M. Koch, D. R. Mariani, and D. Richards, Phys. Rev. Lett. **76**, 892 (1996).
[11] In the experiment [10], by effective ionization one understands either a genuine ionization or excitation above some critical principal quantum number $n_c \approx 110$, which leads to subsequent ionization by electric field outside of the microwave cavity.
[12] K. Sacha and J. Zakrzewski, Phys. Rev. A **55**, 568 (1997).
[13] K. Sacha and J. Zakrzewski, Phys. Rev. A **56**, 719 (1997).
[14] B. V. Chirikov, Phys. Rep. **52**, 265 (1979).
[15] J. G. Leopold and D. Richards, J. Phys. B **19**, 1125 (1986).
[16] J. E. Howard, Phys. Rev. A **46**, 364 (1992).
[17] H. Goldstein, *Classical Dynamics* (Addison-Wesley, Reading, MA, 1980), p. 146.
[18] A. J. Lichtenberg and M. A. Liberman, *Regular and Chaotic Dynamics*, 2nd ed. (Springer, New York, 1992).
[19] The other, more formal way to view the relative importance of Coulomb and microwave perturbations is via the classical scaling properties discussed in [1,8] and used in our work for the discussion of the results.
[20] K. Kaneko and R. J. Bagley, Phys. Lett. **110A**, 435 (1985).
[21] J. Laskar, Physica D **67**, 257 (1993); J. Laskar (private communication).
[22] O. Benson, A. Buchleitner, G. Raithel, M. Arndt, R. N. Mantegna, and H. Walther, Phys. Rev. A **51**, 4862 (1995).
[23] R. S. MacKay, J. D. Meiss, and I. C. Percival, Physica D **13**, 55 (1984).
[24] R. Gębarowski and J. Zakrzewski, Phys. Rev. A **51**, 1508 (1995).
[25] J. C. Day, T. Ehrenreich, S. B. Hansen, E. Horsdal-Pedersen, K. S. Mogensen, and K. Taulbjerg, Phys. Rev. Lett. **72**, 1612 (1994), and references therein.
[26] J. Henkel and M. Holthaus, Phys. Rev. A **45**, 1978 (1992); M. Holthaus, Chaos Solitons Fractals **5**, 1143 (1995), and references therein.